THE JOURNAL OF BIOLOGICAL CHEMISTRY VOL. 283, NO. 19, pp. 12777–12788, May 9, 2008

Characterization of Human SLC4A10 as an Electroneutral Na/HCO_3 Cotransporter (NBCn2) with Cl^- Self-exchange Activity*[S]

Received for publication, September 19, 2007, and in revised form, February 29, 2008 Published, JBC Papers in Press, March 4, 2008, DOI 10.1074/jbc.M707829200

Mark D. Parker[1,2], **Raif Musa-Aziz**[1,2,3], **Jose D. Rojas**[4], **Inyeong Choi**[5], **Christopher M. Daly, and Walter F. Boron**[2,6]

From the Department of Cellular and Molecular Physiology, Yale University, New Haven, Connecticut 06520

The SLC4A10 gene product, commonly known as NCBE, is highly expressed in rodent brain and has been characterized by others as a Na^+-driven Cl-HCO_3 exchanger. However, some of the earlier data are not consistent with Na^+-driven Cl-HCO_3 exchange activity. In the present study, northern blot analysis showed that, also in humans, NCBE transcripts are predominantly expressed in brain. In some human NCBE transcripts, splice cassettes A and/or B, originally reported in rats and mice, are spliced out. In brain cDNA, we found evidence of a unique partial splice of cassette B that is predicted to produce an NCBE protein with a novel C terminus containing a protein kinase C phosphorylation site. We used pH-sensitive microelectrodes to study the molecular physiology of human NCBE expressed in *Xenopus* oocytes. In agreement with others we found that NCBE mediates the 4,4′-diisothiocyanato-stilbene-2,2′-disulfonic acid-sensitive, Na^+-dependent transport of HCO_3^-. For the first time, we demonstrated that this transport process is electroneutral. Using Cl^--sensitive microelectrodes positioned at the oocyte surface, we found that, unlike both human and squid Na^+-driven Cl-HCO_3 exchangers, human NCBE does not normally couple the net influx of HCO_3^- to a net efflux of Cl^-. Moreover we found that that the ^{36}Cl efflux from NCBE-expressing oocytes, interpreted by others to be coupled to the influx of Na^+ and HCO_3^-, actually represents a CO_2/HCO_3^--stimulated Cl^- self-exchange not coupled to either Na^+ or net HCO_3^- transport. We propose to rename NCBE as the second electroneutral Na/HCO_3 cotransporter, NBCn2.

* This work was supported, in whole or in part, by National Institutes of Health Grant NS18400. The costs of publication of this article were defrayed in part by the payment of page charges. This article must therefore be hereby marked "*advertisement*" in accordance with 18 U.S.C. Section 1734 solely to indicate this fact.

[S] The on-line version of this article (available at http://www.jbc.org) contains supplemental material including Table 1 and Figs. 1–4.

The nucleotide sequence(s) reported in this paper has been submitted to the GenBank™/EBI Data Bank with accession number(s) AY376402.

[1] Both authors contributed equally to this work.

[2] Present address: Dept. of Physiology and Biophysics, Case Western Reserve University School of Medicine, Cleveland, OH 44106.

[3] Supported by American Heart Association Fellowship 0625891T.

[4] Present address: Dept. of Respiratory Care, University of Texas Medical Branch, Galveston, TX 77555.

[5] Present address: Dept. of Physiology, Emory University School of Medicine, Atlanta, GA 30322.

[6] To whom correspondence should be addressed: Dept. of Physiology and Biophysics, Case Western Reserve University School of Medicine, 10900 Euclid Ave., Cleveland, OH 44106. Tel.: 216-368-3400; Fax: 216-368-5586; E-mail: wfb2@case.edu.

The mammalian SLC4 family of solute carriers encompasses 10 functionally diverse proteins including Cl-HCO_3 exchangers, both electrogenic and electroneutral sodium-coupled bicarbonate transporters (NCBTs),[7] and a Na^+/borate cotransporter (for reviews, see Refs. 1 and 2). Electroneutral NCBTs play critical roles in regulating the intracellular pH (pH_i) of neurons (3) and in secreting HCO_3^- across the choroid plexus (4, 5). These activities modulate pH in the surrounding brain extracellular fluid (BECF). Changes in both pH_i and pH_{BECF} can have profound effects on ion channels (*e.g.* the acid-sensing ion channel ASIC; see Ref. 6), neurotransmitter receptors (*e.g.* some γ-aminobutyric acid type A receptors; see Ref. 7), and neurotransmitter transporters (*e.g.* the SLC18 family of vesicular amine transporters; for a review, see Ref. 8), thereby influencing neuronal excitability (9, 10), synaptic transmission (for a review, see Ref. 11), and other parameters. The three mammalian electroneutral NCBTs are commonly known as NBCn1, NDCBE, and NCBE and are encoded, respectively, by the *SLC4A7*, *SLC4A8*, and *SLC4A10* genes.

The characterization of the SLC4A7 gene product (12) as NBCn1 (also known as NBC3) provided the first definitive molecular identification of an electroneutral NCBT (13). NBCn1 functions as a Cl^--independent Na/HCO_3 cotransporter. NBCn1 additionally mediates a Na^+ conductance that is independent of its Na/HCO_3 cotransport activity (13). The poor sensitivity of the transporter to DIDS (12, 13) matches the pharmacological profile of stilbene-insensitive NCBT evident in the basolateral membrane of medullary thick ascending limb epithelia (14, 15) where NBCn1 is known to be expressed.

The SLC4A8 gene product was characterized as a $\underline{N}a^+$-$\underline{d}$riven $\underline{C}$l-$\underline{b}$icarbonate $\underline{e}$xchanger (NDCBE), the first mammalian electroneutral NCBT demonstrated to be Cl^--dependent. The importance of Na^+-driven Cl-HCO_3 exchange activity for regulating pH_i has long been established by physiological means in squid giant axons (16, 17), snail neurons (18), giant barnacle muscle fibers (19), and mammalian neurons (3). NDCBE is markedly different from NBCn1 as it has an absolute dependence on Cl^- countertransport for its Na/HCO_3 cotransport activity.

The first slc4a10 gene product was cloned from a mouse insulinoma cell line (20), and a deletion in the human *SLC4A10*

[7] The abbreviations used are: NCBT, sodium-coupled bicarbonate transporter; pH_i, intracellular pH; DIDS, 4,4′-diisothiocyanato-stilbene-2,2′-disulfonic acid; NCBE/NDCBE, Na^+-driven Cl-bicarbonate exchanger; nt, nucleotide; EGFP, enhanced green fluorescent protein; NMDG, *N*-methyl-D-glucamine; V_m, membrane potential; $[Cl^-]_S$, cell surface $[Cl^-]$; ANOVA, analysis of variance; $[Cl^-]_{Bulk}$, bulk extracellular Cl^- concentration.

gene has been linked to autism (21). In mice, the knock-out of *slc4a10* results in small brain ventricles and a decreased susceptibility to seizure activity (22). The presence or absence of two major splice cassettes in rodent *slc4a10* (23) results in multiple splice variants (23). The SLC4A10 gene product has been named "NCBE" for Na^+-driven Cl-bicarbonate exchanger. However, the data presented in support of this nomenclature, 1) NCBE-mediated ^{22}Na and ^{36}Cl influx, 2) HCO_3^--stimulated ^{36}Cl efflux, and 3) bath Cl^- dependence of NCBE-mediated HCO_3^- influx (20), do not prove NDCBE activity. In the present study, we present evidence that the Na/HCO_3 cotransport activity of SLC4A10 under physiological conditions is independent of any Cl^- countertransport and thus that NCBE in fact normally functions as an electroneutral Na/HCO_3 cotransporter. We recommend that the common name for the SLC4A10 gene product be changed to NBCn2. A preliminary report of this work has appeared in abstract form (24).

EXPERIMENTAL PROCEDURES

cDNA Constructs

Human AE1 cDNA in a *Xenopus* expression vector (AE1·pBSXG1; see Ref. 25) was a kind gift from Dr. Ashley Toye, Bristol University, Bristol, UK. We have previously reported the construction and use of the clones (*a*) rat NBCn1-B·pGH19 (cDNA encoding NBCn1 in the *Xenopus* expression vector pGH19; Ref. 13), (b) human NDCBE·pGH19 (26), (*c*) human NBCe1-A-EGFP·pGH19 (NBCe1-A with a C-terminal enhanced green fluorescent protein tag; Ref. 27), and (*d*) squid NDCBE·TOPO (under the control of a T7 promoter; Ref. 28).

NCBE·TOPO—Primers were designed against the 5′- and 3′-untranslated regions of the human brain *SLC4A10* cDNA sequence (GenBank™ DNA accession number AB040457): sense,5′-GCAAGGTGCTTATTCCAGAGGCGTTAC-3′ (nucleotides (nts) 61–87 of AB040457 where the start codon is at nts 93–95); antisense, 5′-TGCTTTGGGGAATCAGCTTCT-AGAGTG-3′ (nts 3361–3387 of AB040457 where the termination codon is at nts 3357–3359). Full-length NCBE cDNA products obtained by PCR from a human Marathon kidney cDNA library (Clontech) were subcloned into the TOPO2.1 vector (Invitrogen) according to the manufacturer's instructions. The fidelity of the clones was confirmed by automated DNA sequencing performed by the Keck Facility at Yale.

NCBE·pGH19—For expression in *Xenopus* oocytes, we subcloned NCBE into pGH19. NCBE cDNA (including 32 nts of 5′-untranslated region and 28 nts of 3′-untranslated region) was amplified by PCR from NCBE·TOPO to include 5′ EcoRV and 3′ HindIII restriction sites (underlined) using the forward PCR primer 5′-CGAAGGATATCGCAAGGTGCTTATTC-CAG-3′ and the reverse PCR primer 5′-CGAAGAAGCTTATG-CTTTGGGGAATCAGC-3′. The EcoRV-NCBE-HindIII PCR product was ligated into complementary SmaI and HindIII restriction sites in the pGH19 vector. NCBE translation from Met^1 (underlined) was put under the control of a strong Kozak sequence, GCCACCATGG, replacing the natural CAAAA-CATGG context using the QuikChange mutagenesis kit (Stratagene, La Jolla, CA) according to the manufacturer's recommendations.

Adding a C-terminal EGFP Tag to Electroneutral NCBT Clones—The construction of NBCn1-B-EGFP·pGH19 (hereafter referred to as NBCn1-EGFP), NCBE-EGFP·pGH19, and NDCBE-EGFP·pGH19 has been described recently (29).

Rapid Amplification of cDNA Ends, Cloning, and Sequencing of NCBE Splice Variants—The methods used to determine the presence and distribution of human NCBE splice variants are outlined in the supplemental data.

Northern Blots

Using the BioPrime DNA labeling system (Invitrogen), we generated a randomly primed 405-nt [^{32}P]dCTP-labeled probe using a cDNA template corresponding to nts 1–405 of the NCBE coding region. Northern blots of mRNAs from multiple human tissues (Clontech "Human," "Human brain II," and "Human brain IV") were hybridized with our probe for 2 h at 68 °C and washed according to the manufacturer's instructions. Results were visualized by autoradiography using Biomax MR film (Eastman Kodak Co.) after a 16-h exposure to the hybridized blots at −80 °C.

cRNA Synthesis and Injection into Xenopus Oocytes

cRNA Synthesis—cDNA constructs in pGH19 were linearized with NotI. AE1·BSXG1 was linearized with HindIII, and squid NDCBE·TOPO was linearized with NheI. Linearized cDNA was purified using the QIAquick PCR purification kit (Qiagen). Capped cRNA was transcribed from the linearized cDNA constructs using the T7 mMessage mMachine kit (Ambion, Austin, TX) according to the manufacturer's recommendations. cRNA was purified and concentrated using the RNeasy MinElute RNA Cleanup kit (Qiagen).

Xenopus Oocyte Isolation—Ovaries were surgically removed from anesthetized frogs in house as described previously (30) or purchased predissected from Nasco (Fort Atkinson, WI). Oocytes were separated by collagenase treatment (30). Stage V-VI oocytes were manually sorted from the total population of separated oocytes and stored in OR3 medium, containing 500 units each of penicillin and streptomycin, at 18 °C until use.

Microinjection of cRNAs—One day after isolation, oocytes were injected either with 25 ng of cRNA (50 nl of a 0.5 ng/nl cRNA solution) or 50 nl of sterile water. Oocytes were stored in OR3 medium at 18 °C for 3–7 days prior to assay.

Solutions

Nominally CO_2/HCO_3^--free "ND96" solution contained 93.5 mM NaCl, 2 mM KCl, 1 mM $MgCl_2$, 1.8 mM $CaCl_2$, and 5 mM HEPES. The pH of the solution was titrated to 7.50 with freshly prepared NaOH so that the final [Na^+] was 96 mM. Our "CO_2/HCO_3^-" solution contained 33 mM $NaHCO_3$ in place of 33 mM NaCl and was equilibrated with a 5% CO_2, 95% O_2 gas mixture. In our butyrate-containing solution, which was nominally free of CO_2/HCO_3^-, 30 mM sodium butyrate replaced 30 mM NaCl. In our Na^+-free "0 Na" solutions, 96 mM *N*-methyl-D-glucamine ($NMDG^+$) replaced 96 mM Na^+. In our Cl^--free "0 Cl" solutions gluconate replaced Cl^-. Solutions containing intermediate concentrations of Cl^- were made by mixing Cl^--containing and Cl^--free solutions in the appropriate ratio. DIDS was supplied as a disodium salt by Sigma and Research Organics, Cleveland, OH.

Electrophysiological Measurements in Xenopus Oocytes

The oocyte chamber and solution flow arrangements have been described recently in detail (27). All experiments were performed at room temperature (~22 °C). Oocytes were superfused with our ND96 solution to allow oocyte pH_i and membrane potential (V_m), as described below, to reach a steady state prior to the application of an experimental solution. All solutions flowed at 4 ml/min.

pH_i Measurements—We simultaneously monitored pH_i (using Hydrogen Ionophore I-Mixture B, catalog number 95293, Fluka Chemical Corp., Ronkonkoma, NY) and V_m of oocytes by impaling cells with two microelectrodes as also described recently in detail (27). A brief summary of the technique is provided in the supplemental material. Data were acquired using customized software.

Surface and Intracellular [Cl^-] Measurements—In some experiments we simultaneously monitored oocyte pH_i, V_m, and cell surface [Cl^-] ([Cl^-]$_S$). We measured [Cl^-]$_S$ using a borosilicate glass microelectrode. After preparing the micropipette as in the pH_i experiments, we used a microforge to break and fire polish the tip to a diameter of 5–10 μm. We then filled the tip with a Cl^--selective liquid membrane (Mixture A, catalog number 24899, Fluka Chemical Corp.) and backfilled with solution containing 150 mM NaCl and 5 mM HEPES, titrated to pH 7.0 with NaOH. Because of the imperfect Cl^-:HCO_3^- selectivity of the liquid membrane mixture, we performed two full calibrations of the electrode before each experiment: one in a series of CO_2/HCO_3^--free ND96 solutions modified to contain [Cl^-] at 5.8, 10, 19, and 30 mM and the other in a series of our CO_2/HCO_3^--containing extracellular solutions modified to contain [Cl^-] at 5.8, 10, 19, and 30 mM. In [Cl^-]$_S$ experiments in which one of the extracellular solutions was Na^+-free, we also performed a full calibration in a series of Na^+-free CO_2/HCO_3^--free ND96 and Na^+-free CO_2/HCO_3^--containing solutions.

We used an ultrafine computer-controlled micromanipulator (model MPC-200 system, Sutter Instrument Co., Novato, CA) to position the tip of the electrode at the oocyte surface and then to further advance it (~40 μm) until we observed a slight dimple in the cell membrane. Periodically during the experiment, the electrode was withdrawn 200–300 μm from the oocyte to recalibrate it at the [Cl^-] of the bulk extracellular fluid. Because the electrode is sensitive to $\log_{10}$[Cl^-], early during the [Cl^-]$_S$ experiments, we reduced extracellular [Cl^-] to 10 mM to maximize electrode sensitivity. A model V3.1 Subtraction Amplifier (Yale University) subtracted the voltage of the bath reference electrode from the voltage of the [Cl^-]$_S$ electrode to produce a voltage due to [Cl^-]$_S$. Data were acquired using customized software.

In some experiments we measured intracellular [Cl^-] and V_m using an approach similar to that in the pH_i experiments except that: 1) the ion-sensitive microelectrode contained the Cl^- rather than the proton mixture, 2) the backfill solution was the one described above for large tipped Cl^--sensitive electrodes, and 3) we calibrated the electrode in a series of CO_2/HCO_3^--free ND96 solutions modified to contain [Cl^-] at 10, 25, 40, 60, and 101 mM.

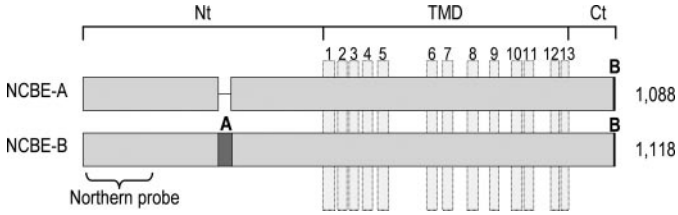

FIGURE 1. **Human splice variants of NCBE.** The *horizontal bars* are scale representations of aligned NCBE protein variants. The putative boundaries of the soluble N terminus (*Nt*), transmembrane domain (*TMD*), and soluble C terminus (*Ct*) are marked along the *top* of the figure. The *numbered, vertical bars* mark positions of individual transmembrane spans. The total length in amino acids of each NCBE is given on the *right-hand side* of the diagram. Human variants NCBE-A (GenBank protein accession number BAB18301) and NCBE-B (reported in the present study, GenBank protein accession number AAQ83632) are shown. The sites of protein variations introduced by the presence or absence of RNA splice cassettes are labeled "*A*" and "*B*." The *brace* identifies the position of the cDNA hybridization sequence used to probe the northern blots presented in Fig. 2.

^{36}Cl Flux Experiments

Isotope—$H^{36}Cl$ (GE Healthcare) was supplied as a 0.2 M stock with an activity of 134 μCi/ml. We prepared a working stock of isotope by diluting the $H^{36}Cl$ with an equal volume of 0.2 M NaOH to create 0.1 M $Na^{36}Cl$.

^{36}Cl Efflux—Detailed assay methods and efflux calculations are described in the supplemental material. In brief, oocytes were preloaded with ^{36}Cl overnight in nominally CO_2/HCO_3^--free "ND96" solution, and efflux was measured twice for each oocyte. The first 30-min efflux period was always in ND96; the second 30-min efflux period was in one of a diverse range of solutions.

Data Analysis—Statistical analyses were performed in Microsoft Excel 1997 (paired and unpaired *t* tests assuming equal variances) and Kaleidagraph version 4.0 (one-way ANOVA with Student-Newman-Keuls multiple comparison posthoc analysis).

RESULTS

Cloning Human NCBE—Using primers specific to the untranslated regions of a published *SLC4A10* transcript from human brain (GenBank accession number AB040457, encoding a variant protein that we call NCBE-A; Fig. 1), we generated a PCR product from a human kidney cDNA library. We subsequently ligated this product into the TOPO vector. DNA sequencing of four independent TOPO clones revealed four full-length cDNAs identical to NCBE-A except for an additional 90 nts corresponding to splice cassette A (Fig. 1). We deposited the sequence of the new human transcript in GenBank (nucleotide accession number AY376402); here we temporarily refer to this longer protein product as NCBE-B (Fig. 1). We performed all functional assays in the present work using NCBE-B.

Human NCBE mRNA Is Widely Distributed in the Brain—Northern blotting of mRNAs prepared from various human organs, using a probe common to NCBE-A and NCBE-B, demonstrated that NCBE transcripts are predominantly expressed in the brain (Fig. 2*A*, lane 2). The major transcript is ~6.3 kb with an additional larger product of ~9.5 kb. We saw no additional bands even with greatly increased periods of film exposure (not shown). Northern blotting of mRNAs pre-

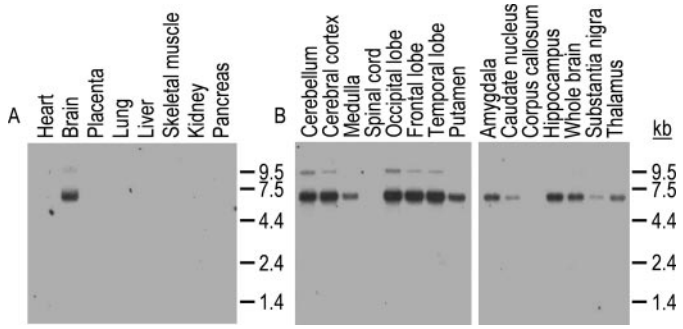

FIGURE 2. **Northern blots of human NCBE.** Multiple tissue northern blots (Clontech) were probed with a ^{32}P-labeled cDNA designed to hybridize with the region of NCBE indicated in Fig. 1. These blots were of human cRNA from various organs (*A*) and human cRNA from various brain regions (*B*).

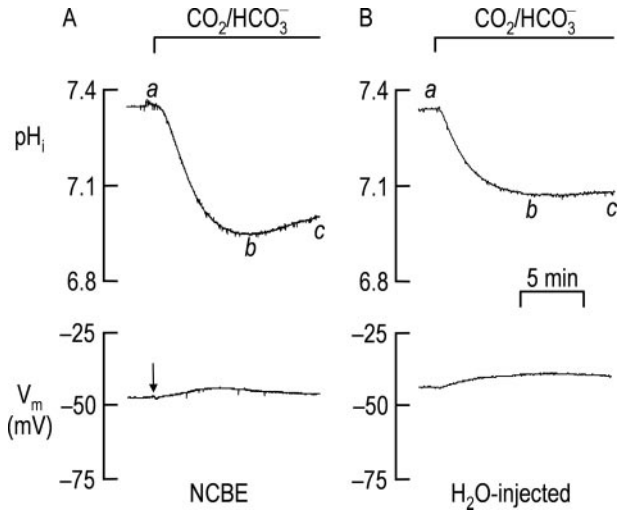

FIGURE 3. **pH_i recovery mediated by NCBE.** Representative traces from experiments in which we simultaneously recorded pH_i and V_m are shown. *A*, NCBE-expressing oocytes. *B*, H_2O-injected oocytes. In both cases, the oocytes were acidified in our CO_2/HCO_3^- solution (segment *ab*). pH_i recovery from the acid load (*bc*) was observed in oocytes expressing NCBE. The application of CO_2/HCO_3^- to NCBE-expressing oocytes did not elicit and rapid changes in V_m (*arrow* in *lower panel*).

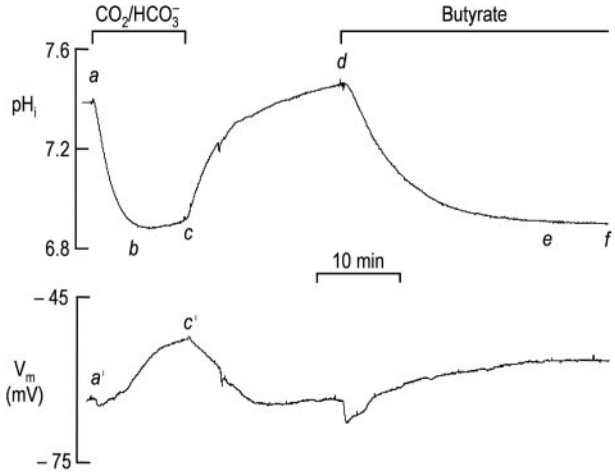

FIGURE 4. **HCO_3^- dependence of pH_i recovery mediated by NCBE.** Shown are representative traces from a series of experiments in which we simultaneously recorded pH_i and V_m in NCBE-expressing oocytes that we acidified either in our CO_2/HCO_3^- solution (segment *ab*) or in our butyrate solution (segment *de*). pH_i recovery from the acid load was only observed when cells were acidified in the presence of extracellular HCO_3^- (*bc versus ef*). The unusually large depolarization in segment *a′c′* of this experiment was typical for this particular set of experiments but not representative of NCBE expressing oocytes as a whole (see Fig. 3 and Figs. 5–8) and likely reflects an unusually tight membrane (as evidenced by the relatively negative resting V_m) in the presence of the usual, small, endogenous acid-stimulated current.

pared from various regions of human brain revealed a widespread distribution of NCBE (Fig. 2*B*). NCBE mRNA was poorly represented in the spinal cord (Fig. 2*B*, *left panel*, *lane 4*) and corpus callosum (Fig. 2*B*, *right panel*, *lane 3*), although we note that longer exposures of the blot demonstrated that NCBE transcripts are not entirely absent in these tissues (not shown).

Human NCBE Has Multiple Splice Variants—Here we determined which of the multiplicity of NCBE splice variants, known to be expressed in rodents (23), could also be detected in a human brain cDNA library. The results of this survey, including the description of a novel C-terminal splice variant with a consensus protein kinase C phosphorylation site, are presented in the supplemental data.

Like NBCn1 and Like NDCBE, NCBE Mediates Electroneutral Na^+-dependent HCO_3^- Influx into Xenopus Oocytes—Our laboratory has demonstrated previously that the pH_i of oocytes expressing NCBTs is able to recover from a CO_2-induced acid load only in the presence of extracellular HCO_3^- and Na^+ (*e.g.* see Ref. 31).

In the present study, we found that pH_i recovery (Fig. 3*A*, *upper panel*, segment *bc*) from a CO_2-induced acid load (*ab*) is a characteristic of *Xenopus* oocytes expressing NCBE (mean $dpH_i/dt = 14 \pm 1 \times 10^{-5}$ pH units/s, $n = 82$) but not of oocytes injected with H_2O (Fig. 3*B*, *upper panel*; mean $dpH_i/dt = 3 \pm 1 \times 10^{-5}$ pH units/s, $n = 41$). Furthermore this pH_i recovery of NCBE-expressing oocytes requires HCO_3^- and is not merely a response to the fall in pH_i because oocytes that were acidified in our butyrate solution failed to exhibit a pH_i recovery (Fig. 4, *upper panel*, segment *ef*; mean $dpH_i/dt = 1 \pm 1 \times 10^{-5}$ pH units/s, $n = 6$). In some experiments on the same oocytes, we monitored pH_i recovery from a CO_2-induced acid load either prior to (as represented in Fig. 4, *upper panel*, segment *bc*) or subsequent to (not shown) butyrate exposure. In this way we verified functional expression of NCBE in these cells (mean $dpH_i/dt = 18 \pm 3 \times 10^{-5}$ pH units/s, $n = 4$). Note that the application of CO_2/HCO_3^- to NCBE-expressing oocytes did not elicit any rapid changes in V_m (*arrows* in Fig. 3 and Fig. 4, *lower panels*), indicating that the HCO_3^--dependent pH_i recovery is electroneutral.

To investigate cation dependence of HCO_3^- transport mediated by NCBE, we acidified NCBE-expressing oocytes (Fig. 5, *upper panel*, *ab*) in a Na^+-free CO_2/HCO_3^- solution in which $NMDG^+$ entirely replaced Na^+. The pH_i of NCBE-expressing oocytes was unable to recover from this acid load (*bc*; mean $dpH_i/dt = -2 \pm 1 \times 10^{-5}$ pH units/s, $n = 6$) under these conditions. Replacing bath $NMDG^+$ with Li^+ did nothing further to permit HCO_3^- transport (*cd*; mean $dpH_i/dt = -4 \pm 3 \times 10^{-5}$ pH units/s, $n = 6$). However, subsequently replacing bath Li^+ with Na^+ initiated a substantial pH_i recovery (*de*; mean $dpH_i/dt = 45 \pm 6 \times 10^{-5}$ pH units/s, $n = 6$). The removal of bath Na^+ did not elicit a substantial acidification (which would have been consistent with a reversal in the direction of transport). Instead when Na^+ was removed and Li^+ restored, the

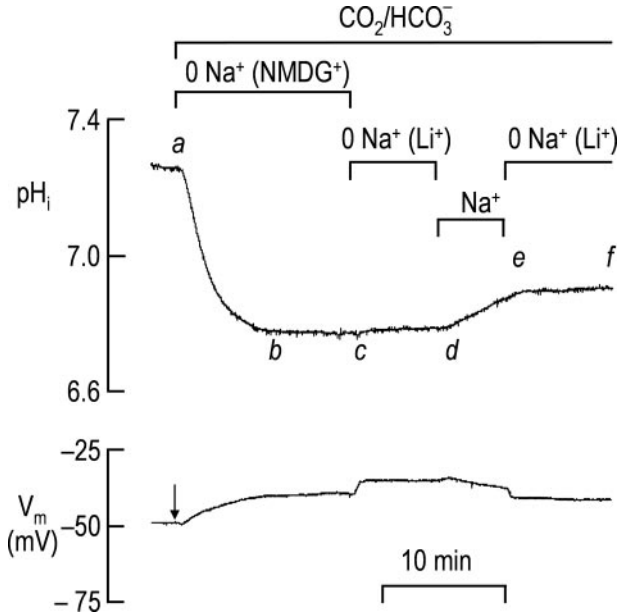

FIGURE 5. **Na^+ dependence of NCBE-mediated HCO_3^- transport (Part I).** Shown is a representative trace from a series of experiments in which we simultaneously recorded pH_i and V_m in NCBE-expressing oocytes that we acidified in a CO_2/HCO_3^- solution (segment *ab*) in which $NMDG^+$ fully replaced Na^+. pH_i recovery from the acid load did not occur in this solution (*bc*) or in a Li^+-containing solution (*cd*). pH_i recovery was only permitted when Na^+ was restored to the bath (*de*). pH_i recovery ceased again upon subsequent removal of bath Na^+ (*ef*). The application of CO_2/HCO_3^- to NCBE-expressing oocytes did not elicit and rapid changes in V_m (*arrow* in *lower panel*).

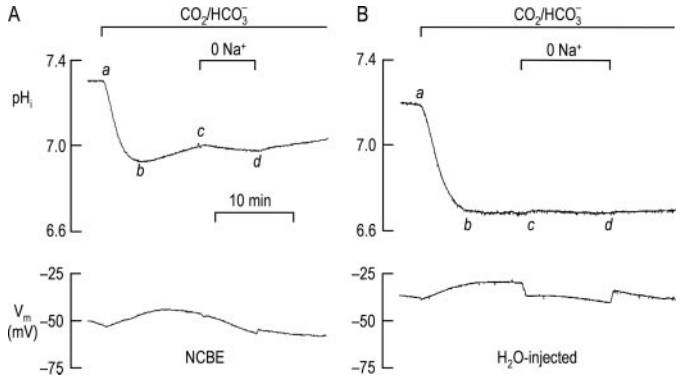

FIGURE 6. **Na^+ dependence of NCBE-mediated HCO_3^- transport (Part II).** Shown are representative traces from a series of experiments in which we simultaneously recorded pH_i and V_m in NCBE-expressing oocytes that we acidified in CO_2/HCO_3^--containing solutions (segments *ab*). *A*, NCBE-expressing oocyte. *B*, H_2O-injected oocyte. In the presence of Na^+, pH_i recovery from the acid load occurred in oocytes expressing NCBE (segment *bc* in *A*; $12 \pm 1 \times 10^{-5}$ pH units/s, $n = 46$) but not H_2O-injected oocytes (segment *bc* in *B*; $4 \pm 1 \times 10^{-5}$ pH units/s, $n = 24$). In both panels, removal of bath Na^+ caused pH_i to fall slowly (*cd*) as summarized in the text.

pH_i recovery merely ceased (*ef*; $dpH_i/dt = -2 \pm 2 \times 10^{-5}$ pH units/s, $n = 4$).

The stability of pH_i in segment *ef* in Fig. 5, *upper panel*, does not rule out the possibility that NCBE can operate in reverse inasmuch as Li^+ might behave as a blocker. Therefore, we performed a separate series of experiments, typified by those presented in Fig. 6, in which we acid-loaded with CO_2/HCO_3^- (*ab*), monitored the pH_i recovery (*bc*), and then replaced bath Na^+ with $NMDG^+$ (*cd*). We found that the mean segment *cd* rate of acidification in NCBE-expressing oocytes was $-7 \pm 1 \times 10^{-5}$ pH units/s ($n = 46$) compared with $-4 \pm 1 \times 10^{-5}$ pH units/s ($n = 24$) for H_2O-injected oocytes. Although the mean acidification rate was significantly greater in NCBE-expressing than in H_2O-injected cells ($p < 0.01$, unpaired one-tailed *t* test assuming equal variances), the difference was not substantial. Other Na^+-coupled HCO_3^- transporters are also noted to reverse poorly (16, 26).

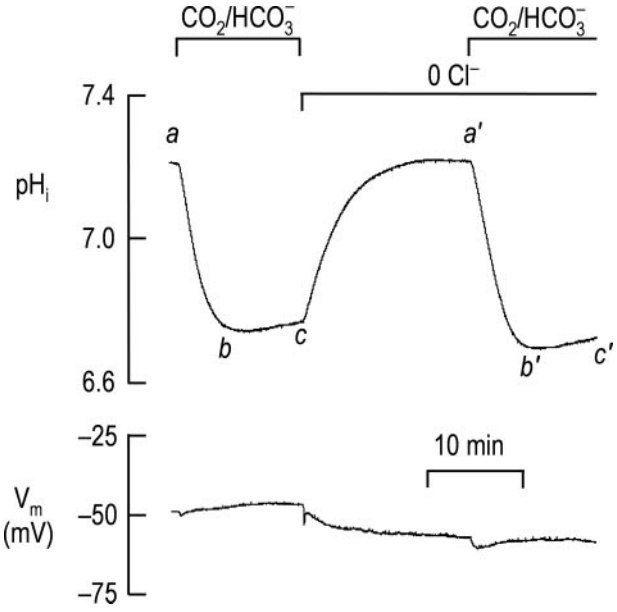

FIGURE 7. **Extracellular Cl^- independence of NCBE-mediated HCO_3^- transport.** A representative trace from a series of experiments in which we simultaneously recorded pH_i and V_m in NCBE-expressing oocytes that we twice acidified in CO_2/HCO_3^- solutions, once in the presence and once in the absence of bath Cl^-. In half of the experiments and in the trace shown here, the oocyte was acidified initially in a Cl^--containing CO_2/HCO_3^- solution (segment *ab*) and subsequently in a Cl^--free CO_2/HCO_3^- solution (segment *a′b′*). In the other half of the experiments, we reversed the order of the two CO_2/HCO_3^- pulses (not shown); oocytes were acidified initially in a Cl^--free CO_2/HCO_3^- solution and subsequently in a Cl^--containing CO_2/HCO_3^- solution. The mean pH_i recovery rate from the acid load was identical in both solutions (*bc versus b′c′*).

Where indicated, we performed some of the subsequent experiments in this study on oocytes expressing NCBE-EGFP to confirm NCBE expression in individual oocytes prior to, or following, the electrophysiological experiment (27). To examine whether the addition of a C-terminal EGFP tag interferes with the HCO_3^- transport function of NCBE, we compared the rate of pH_i recovery of oocytes expressing NCBE with that of oocytes expressing NCBE-EGFP in our CO_2/HCO_3^- solution. In side-by-side experiments, we found that the untagged protein mediates oocyte pH_i recovery ($dpH_i/dt = 10 \pm 1 \times 10^{-5}$ pH units/s, $n = 6$; not shown) at a rate that is indistinguishable from that of NCBE-EGFP (not shown; $dpH_i/dt = 11 \pm 2 \times 10^{-5}$ pH units/s, $n = 6$; $p = 0.72$, unpaired two-tailed *t* test assuming equal variances).

To investigate whether the HCO_3^- transport mediated by NCBE in oocytes required extracellular Cl^-, we exposed NCBE-EGFP-expressing oocytes to two serial pulses of CO_2/HCO_3^-, either the first or second of which, in alternating order, lacked extracellular Cl^- (68 mM sodium gluconate replaced 68 mM NaCl). We found that the rate of pH_i recovery from the CO_2-induced acid load is not changed ($p = 0.89$, paired two-

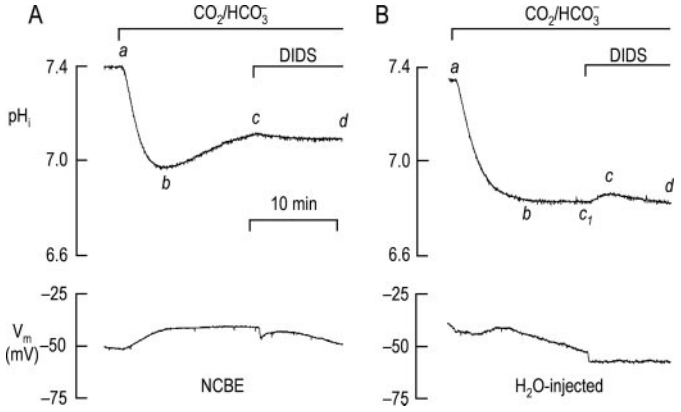

FIGURE 8. **DIDS blockade of NCBE-mediated HCO_3^- transport.** Shown are representative traces from a series of experiments in which we simultaneously recorded pH_i and V_m. *A*, NCBE-expressing oocytes. *B*, H_2O-injected oocytes. In both cases, we acidified the cells in a CO_2/HCO_3^--containing solution (segments *ab*). pH_i recovery from the acid load occurred in oocytes expressing NCBE (segment *bc* in *A*; $17 \pm 2 \times 10^{-5}$ pH units/s, $n = 14$) but not H_2O-injected oocytes (segment bc_1 in *B*; $1 \pm 1 \times 10^{-5}$ pH units/s, $n = 7$). Addition of 200 μM DIDS (Sigma) to the bath caused the pH_i of both populations of oocytes to fall slowly (*cd*). In many oocytes, we observed a brief alkalinization upon DIDS application, such as that shown in *B*, segment c_1c.

tailed *t* test) whether extracellular Cl^- is present (Fig. 7, *upper panel*, *bc*; mean $dpH_i/dt = 9 \pm 2 \times 10^{-5}$ pH units/s, $n = 6$; rate measured at average $pH_i = 6.77 \pm 0.08$) or absent (Fig. 7, *upper panel*, *b′c′*; mean $dpH_i/dt = 10 \pm 1 \times 10^{-5}$ pH units/s, $n = 6$; rate measured at average $pH_i = 6.77 \pm 0.09$).

Like NBCn1 and Like NDCBE, NCBE Is Blocked by DIDS—We serially exposed NCBE-expressing (or H_2O-injected) oocytes to our CO_2/HCO_3^- solution followed by the CO_2/HCO_3^- solution containing 200 μM DIDS. As we have shown, pH_i in NCBE-expressing oocytes recovered from the CO_2-induced acid load (Fig. 8*A*, *upper panel*, *bc*). The application of DIDS blocked this recovery (*cd*; mean $dpH_i/dt = -8 \pm 1 \times 10^{-5}$ pH units/s, $n = 14$). Again as expected, pH_i in H_2O-injected oocytes failed to recover from the CO_2-induced acidification (Fig. 8*B*, *upper panel*, *bc*). However, the subsequent application of DIDS caused pH_i to fall (Fig. 8*B*, *upper panel*, *cd*; mean $dpH_i/dt = -8 \pm 2 \times 10^{-5}$ pH units/s, $n = 7$). Note that the segment *cd* acidification rates were indistinguishable in NCBE-expressing *versus* H_2O-injected cells ($p = 0.53$, unpaired two-tailed *t* test assuming equal variances).

Like NBCn1 but Unlike NDCBE, NCBE Does Not Mediate a Net Efflux of Cl^-—We expressed NCBE-EGFP in *Xenopus* oocytes. As positive controls, we used oocytes expressing AE1, human NDCBE-EGFP, and squid NDCBE. As negative controls, we used oocytes expressing NBCn1-EGFP as well as H_2O-injected oocytes. Using sharp Cl^--selective microelectrodes, we found that the mean intracellular $[Cl^-]$ of all six populations of oocytes, measured with the oocytes exposed to the ND96 solution, is ~40 mM (Table 1, column 2). This value, which is similar to that reported by others for oocytes (32, 33), is considerably higher than the equilibrium value of 23 mM (computed using the mean measured V_m of −37 mV)[8] and indicates that oocytes have one or more active Cl^- uptake mechanisms (*e.g.*

[8] This population included NCBn1-expressing oocytes, which have a relatively positive V_m.

TABLE 1

Mean values for resting $[Cl^-]_i$ and $[Cl^-]_S$

$[Cl^-]_i$ in column 2 is the steady-state value of oocytes bathed in ND96 solution ($[Cl^-]_{Bulk}$ = 101 mM). We continuously monitored $[Cl^-]_i$ while switching $[Cl^-]_{Bulk}$ from 101 to 10 mM. The $\Delta[Cl^-]_i$ value in column 3 reflects the change in $[Cl^-]_i$ 5 min after the switch to the HEPES-buffered 10 mM Cl^- solution (*i.e.* corresponding to the time just before the switch to CO_2/HCO_3^- in Fig. 9). In the NCBE-expressing oocytes, we followed the 5-min exposure to 10 mM Cl^- (summarized in column 3) with a 15-min exposure to 0 mM Cl^- ($\Delta[Cl]_i = -1 \pm 1$ mM, $n = 4$; not shown). Finally the $[Cl^-]_S$ data in column 4, obtained on the oocytes shown in Figs. 9 and 10, represent the surface $[Cl^-]$ just before the switch from the HEPES-buffered 10 mM Cl^- solution to the CO_2/HCO_3^--buffered 10 mM Cl^- solution. hNDCBE, human NDCBE; sqNDCBE, squid NDCBE.

	$[Cl^-]_i$ ($[Cl^-]_{Bulk}$ = 101 mM)	$\Delta[Cl^-]_i$ ($[Cl^-]_{Bulk}$ = 10 mM)	$[Cl^-]_S$ ($[Cl^-]_{Bulk}$ = 10 mM)
	mM	*mM*	*mM*
AE1	37 ± 1 (n = 4)	−1 ± 1 (n = 4)	21 ± 1 (n = 10)
hNDCBE	39 ± 3 (n = 4)	−2 ± 1 (n = 4)	18 ± 2 (n = 9)
sqNDCBE	38 ± 2 (n = 4)	−3 ± 2 (n = 3)	20 ± 1 (n = 9)
NBCn1	42 ± 4 (n = 6)	−1 ± 1 (n = 3)	22 ± 2 (n = 7)
H_2O	39 ± 2 (n = 7)	−2 ± 2 (n = 3)	19 ± 1 (n = 6)
NCBE	40 ± 3 (n = 7)	−1 ± 1 (n = 4)	22 ± 1 (n = 8)

Na/K/2Cl cotransport). For all oocyte populations, $[Cl^-]_i$ rapidly reached a new steady-state value after we exposed the cells to a HEPES-buffered 10 mM Cl^- solution (Table 1, column 3). Cells were not substantially Cl^- depleted by a 5-min exposure to the 10 mM Cl^- solution (Table 1, column 3 *versus* column 2). Even after a subsequent 15-min exposure to a Cl^--free HEPES-buffered solution, the $[Cl^-]_i$ of NCBE-expressing oocytes was not significantly lowered (not shown; $n = 4$; $p = 0.40$, paired one-tailed *t* test).

Fig. 9 shows a series of representative experiments in which we used a blunt tipped Cl^--selective microelectrode to monitor the $[Cl^-]_S$ in each of the six populations of oocytes. Each experiment began with the oocyte exposed to the ND96 solution. Because Cl^--sensitive electrodes are sensitive to the $\log_{10}[Cl^-]$, we reduced the bulk extracellular Cl^- concentration ($[Cl^-]_{Bulk}$) to 10 mM to enhance the sensitivity of the electrodes to changes in $[Cl^-]_S$. This reduction in $[Cl^-]_{Bulk}$ presumably enhanced the net Cl^- efflux from the oocytes. Indeed we found that the mean $[Cl^-]_S$ of oocytes exposed to a HEPES-buffered 10 mM Cl^- solution was ~20 mM (see Table 1, column 5); the ~10 mM difference between $[Cl^-]_{Bulk}$ and $[Cl^-]_S$ is a semiquantitative index of the net Cl^- efflux analogous to the outward $[Cl^-]$ gradient that others have measured using self-referencing ion-selective electrodes (34).

We next replaced the HEPES-buffered 10 mM Cl^- solution with a solution of identical $[Cl^-]_{Bulk}$ but now buffered with CO_2/HCO_3^-. If the oocyte is expressing a membrane protein that exchanges extracellular HCO_3^- for intracellular Cl^-, then this switch to CO_2/HCO_3^- ought to enhance the net efflux of Cl^-, which we would detect as a transient increase in $[Cl^-]_S$. For the positive controls, AE1, human NDCBE-EGFP, and squid NDCBE, applying CO_2/HCO_3^- indeed caused a transient increase in $[Cl^-]_S$ followed by a slow decrease as represented in Fig. 9, *A–C*, and summarized in Fig. 10*A*. For the negative controls, NBCn1-EGFP and H_2O, applying CO_2/HCO_3^- caused a decrease in $[Cl^-]_S$ as represented in Fig. 9, *D* and *E*, and summarized in Fig. 10*A*. This decrease implies that that CO_2/HCO_3^- (perhaps by lowering pH_i) reduces the net efflux of Cl^-. Finally for NCBE-EGFP, applying CO_2/HCO_3^- caused a decrease in $[Cl^-]_S$ (Figs. 9*F* and 10*A*) as we observed for the

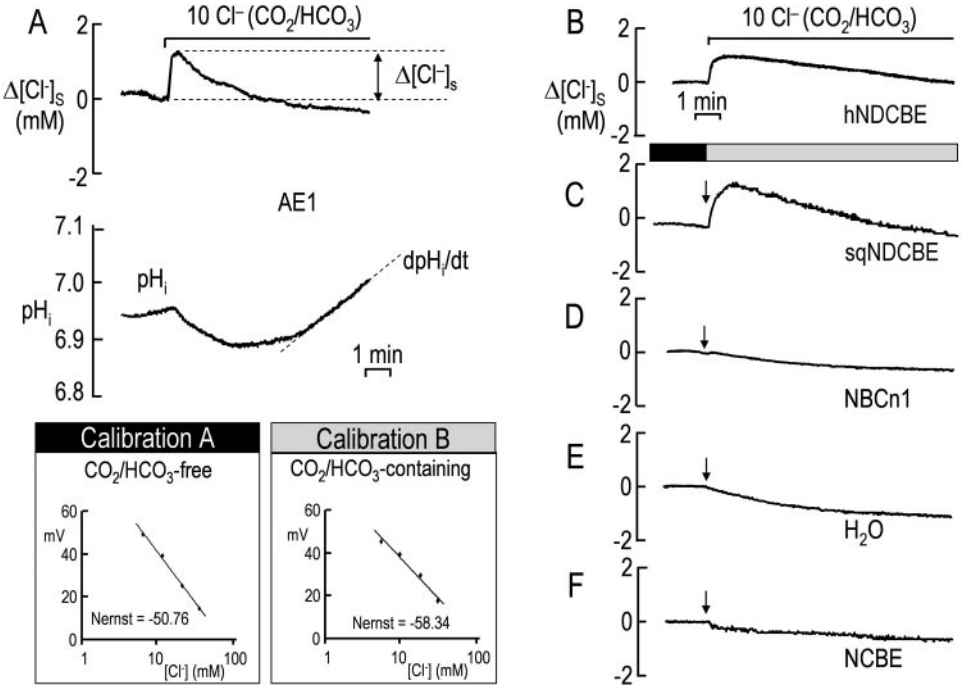

FIGURE 9. **Perturbations of surface [Cl^-] in response to the application of CO_2/HCO_3^-.** Shown are representative traces from a series of experiments in which we simultaneously monitored [Cl^-] at the oocyte surface ([Cl^-]$_S$) as well as pH_i and V_m as we exposed cells to a solution containing CO_2/HCO_3^- (instant of solution change marked with *arrows* in *panels C–F*). Representative [Cl^-]$_S$ measurements are shown for oocytes heterologously expressing AE1 (*A*, *upper panel*), human NDCBE-EGFP (*B*), squid NDCBE (*sqNDCBE*) (*C*), NBCn1-EGFP (*D*), nothing (*i.e.* H_2O-injected oocytes) (*E*), and NCBE-EGFP (*hNDCBE*) (*F*). Before each experiment, the [Cl^-]$_S$ electrode was calibrated once in the absence of CO_2/HCO_3^- (represented in the *inset*, *Calibration A*; this calibration was applied to the portion of the [Cl^-]$_S$ trace gathered in the absence of CO_2/HCO_3^- (*black bars*)), and once in the presence of CO_2/HCO_3^- (represented in the *inset*, *Calibration B*; this calibration was applied to the portion of the [Cl^-]$_S$ trace gathered in the presence of CO_2/HCO_3^- (*gray bars*)). Average [Cl^-]$_S$ and pH_i data for all populations of oocytes are provided in Fig. 10. A representative pH_i trace is provided for a cell expressing AE1 (*A*, *lower panel*).

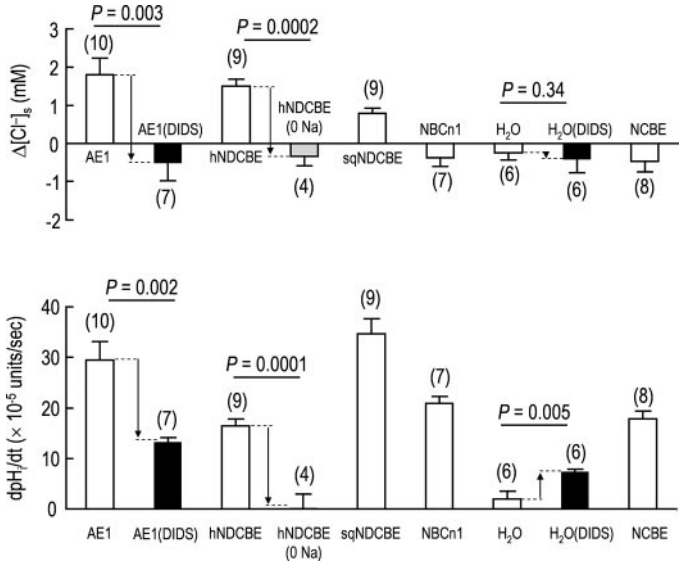

FIGURE 10. **Average maximal changes in [Cl^-]$_S$ and average rates of pH_i recovery in oocytes exposed to CO_2/HCO_3^-.** Shown are mean data from experiments such as those presented in Fig. 9 in which we simultaneously monitored [Cl^-]$_S$ (*A*) and pH_i (*B*) of oocytes during exposure to CO_2/HCO_3^- solution. *Black bars* are data gathered from oocytes that had been preincubated with 200 μM DIDS for 1 h prior to assay. *Gray bars* are data gathered from oocytes that were exposed to CO_2/HCO_3^- solution in the absence of bath Na^+. Values are means ± S.E. with number of oocytes in *parentheses*. *hNDCBE*, human NDCBE; *sqNDCBE*, squid NDCBE.

negative controls. These differences are not explained by substantial variations among oocyte populations in either (*a*) [Cl^-]$_i$ following exposure to our HEPES-buffered 10 mM Cl^- solution (Table 1, column 3; $p = 0.36$, one-way ANOVA) or (*b*) the steady-state [Cl^-]$_S$ in this same solution (Table 1, column 4; $p = 0.30$, one-way ANOVA).

In these same experiments, we concurrently monitored pH_i (represented for AE1 in Fig. 9*A*, *middle panel*) to confirm the presence (or absence in the case of H_2O-injected cells) of the pH_i recovery that reflects net HCO_3^- uptake. Fig. 10*B* summarizes the mean rates of pH_i recovery rates. The presence of a pH_i recovery for NCBE-EGFP oocytes and the lack of a [Cl^-]$_S$ spike show that NCBE does not couple HCO_3^- uptake to the net efflux of Cl^- in the presence of 10 mM extracellular Cl^-.

As a control, we verified that pretreating AE1 oocytes with DIDS for 1 h, a treatment known to irreversibly block about half of ^{36}Cl efflux through mouse AE1 (35), reduces both the size of the [Cl^-]$_S$ spike and the rate of pH_i recovery (Fig. 10, *black bars*). Thus, our approach for monitoring [Cl^-]$_S$ appears to be appropriate for assessing net Cl^- efflux coupled to HCO_3^- influx.

Finally using an experimental approach similar to that presented in Fig. 5, when we first exposed NDCBE-expressing oocytes to CO_2/HCO_3^- in the continued absence of Na^+, we observed neither a [Cl^-]$_S$ spike nor a pH_i recovery (Fig. 10, *fourth bar*). Thus, our approach for monitoring [Cl^-]$_S$ appears to be appropriate for assessing net Cl^- efflux coupled to Na^+ and HCO_3^- influx.

Unlike NDCBE, NCBE Mediates a ^{36}Cl Efflux That Is Na^+-independent—Others have reported that, in oocytes, NCBE mediates the efflux of ^{36}Cl when Na^+ and HCO_3^- are present in the extracellular fluid (20).

Comparing the ^{36}Cl efflux from oocytes bathed in ND96 with those bathed in CO_2/HCO_3^- solution, we found that, in the presence of bath Na^+, CO_2/HCO_3^- stimulates ^{36}Cl efflux from oocytes expressing NDCBE-EGFP (Fig. 11*A*, *bar F versus bar B*; $p < 0.0001$, one-way ANOVA with Student-Newman-Keuls posthoc analysis as are all statistics quoted in this section) or NCBE-EGFP (Fig. 11*B*, *bar F versus bar B*; $p < 0.0001$) but not from oocytes that were injected with H_2O (Fig. 11*C*, *bar F versus bar B*; $p = 0.995$). These results are in agreement with previous reports (20, 26).

We found that the CO_2/HCO_3^--stimulated ^{36}Cl efflux from NDCBE-expressing oocytes requires bath Na^+ (Fig. 11*A*, *bar G*

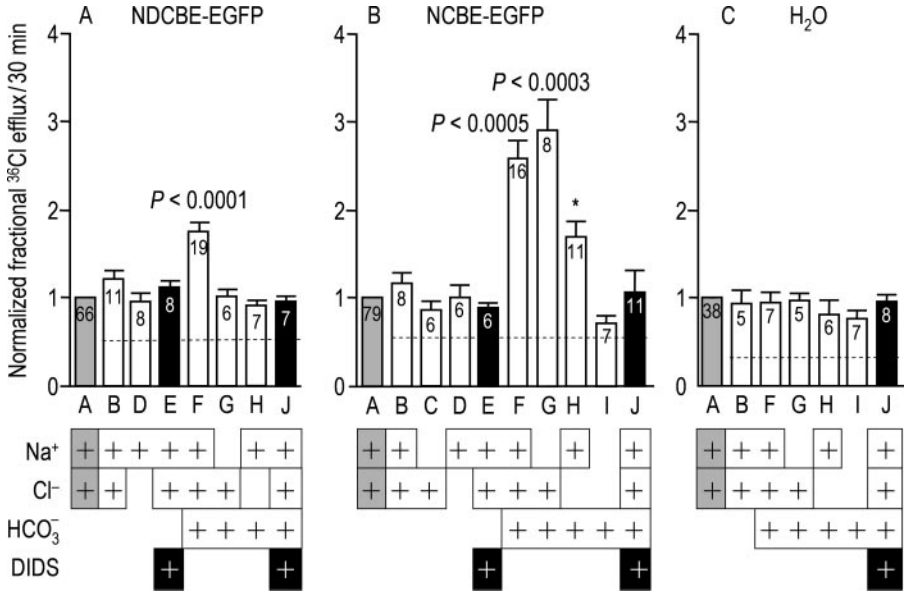

FIGURE 11. **Efflux of ^{36}Cl from oocytes.** *A*, NDCBE-EGFP. *B*, NCBE-EGFP. *C*, oocytes injected with H_2O. The values on the *ordinate* represent the fractional efflux of ^{36}Cl (mean ± S.E.) measured over one of two 30-min collection periods. In each panel, the *gray "A" bar* represents the normalized value for the first collection period in ND96 solution. The *white bars* represent data from a second collection period (*bars B–H*), normalized to the value in the corresponding first collection period. The *horizontal dashed line* represents the average estimated normalized background (*i.e.* "zero" efflux) value for the second period. We calculated that, at the beginning of the first efflux period (*i.e.* before *gray bar*), NDCBE-expressing oocytes contained 553 ± 30 cpm ($n = 66$), NCBE-expressing oocytes contained 774 ± 30 cpm ($n = 34$), and H_2O-injected oocytes contained 325 ± 48 cpm ($n = 27$). For a given panel, these initial cpm values did not differ significantly among oocytes subsequently assigned to groups B–J (one-way ANOVA, $p > 0.10$ in all cases). The fractional loss of ^{36}Cl during the first 30-min efflux period in ND96 (*i.e.* during *gray bar*) was 13 ± 1% ($n = 66$) for NDCBE-expressing oocytes, 9 ± 1% ($n = 79$) for NCBE-expressing oocytes, and 33 ± 3% ($n = 38$) for H_2O-injected oocytes. For a given panel, these first period fractional losses did not differ significantly among oocytes subsequently assigned to groups B–J (one-way ANOVA, $p > 0.08$ in all cases). *Bars* marked with *p* values are significantly different from all *unmarked bars* within that panel (one-way ANOVA with Student-Newman-Keuls posthoc analysis). In *B*, *bars F* and *G* are not significantly different from each other ($p = 0.247$). *, in *B*, *bar H* is significantly different from *bars F* ($p = 0.0004$), *G* ($p = 0.0002$), and *I* ($p = 0.028$) but not *bar J* ($p = 0.05$) or bars *B–E* ($p > 0.07$). *Unmarked bars* are not significantly different from each other ($p > 0.71$).

versus bar F; $p < 0.0001$) and is blocked by 200 μM DIDS (Fig. 11*A*, *bar J versus bar F*; $p < 0.0001$) also in agreement with a similar assay for NDCBE activity (26). The CO_2/HCO_3^--stimulated ^{36}Cl efflux from NDCBE-expressing oocytes also required bath Cl^- (Fig. 11*A*, *bar H versus bar F*; $p < 0.0001$). These data are the first direct demonstration that NDCBE engages in Cl-Cl exchange under near physiological conditions.

As is the case with NDCBE-expressing oocytes, we found that the CO_2/HCO_3^--stimulated ^{36}Cl efflux from NCBE-expressing oocytes is blocked by 200 μM DIDS (Fig. 11*B*, *bar J versus bar F*; $p < 0.0001$) and requires bath Cl^- (Fig. 11*B*, *bar H versus bar F*; $p = 0.0004$). However, the CO_2/HCO_3^--stimulated ^{36}Cl efflux did not require bath Na^+ in NCBE-expressing oocytes (Fig. 11*B*, *bar G versus bar C* ($p < 0.0001$) and *bar G versus bar F* ($p = 0.247$)) in contrast to NDCBE-expressing oocytes. In the absence of bath Na^+, the additional removal of bath Cl^- negated the CO_2/HCO_3^--stimulated ^{36}Cl efflux (Fig. 11*B*, *bar I versus bar G*; $p < 0.0001$) and demonstrates that, at least in the absence of bath Na^+, NCBE engages in CO_2/HCO_3^--stimulated Cl-Cl exchange. A curious observation in NCBE-expressing oocytes is that, in the absence of bath Cl^-, adding bath Na^+ now stimulated a CO_2/HCO_3^--dependent ^{36}Cl efflux (Fig. 11*B*, *bar I versus bar H*; $p < 0.03$). This flux, which is only about one-third as large as the ^{36}Cl flux that we observed in the presence of bath Cl^- under near physiological conditions (Fig. 11*B*, *bar F*), is consistent with a small amount of Na^+-driven Cl-HCO_3 exchange activity but only in the nonphysiological state in which extracellular Cl^- is totally absent.

DISCUSSION

The purpose of this study was to clarify the distribution and molecular mechanism of the human SLC4A10 gene product toward a better understanding of its physiological purpose. Prior to the present report, nearly all of the work has concentrated on rodent orthologs of the transporter.

NCBE mRNA Is Widely Distributed in Human Brain

Our northern blots of human RNA demonstrated that, among the sources tested, NCBE is predominantly expressed in the brain (Fig. 2*A*). These data accord with rat northern blot data that show highest expression in the brain but lower expression in ileum, kidney, pituitary tissue (20), and spleen (23). Those authors and others (36) detected, by northern blot and *in situ* hybridization, a broad distribution of NCBE transcripts throughout the brains of adult rats (20, 23) and embryonic mice (36). Our Northern blotting study showed a similarly widespread expression of NCBE transcripts throughout the adult human brain (Fig. 2*B*). To our knowledge, our study is the first to identify the presence, in any species, of NCBE transcripts in the amygdala, caudate nucleus, putamen, and substantia nigra. Furthermore our study is the first to identify the corpus callosum and spinal cord as being regions of particularly weak NCBE expression. On the other hand, Hubner *et al.* have detected NCBE transcripts, by *in situ* hybridization, in the spinal cords of embryonic mice (36). Although the reason for this disparity is unresolved, we propose differences in species, developmental stage, and/or RNA preparation to be relevant considerations. The mRNA of another electroneutral Na^+-coupled HCO_3^- transporter, NDCBE, is also notably absent from human spinal cord (26).

Multiple Splice Variants of NCBE Are Detected in Human cDNA Libraries

A discussion of the presence and distribution of multiple human NCBE splice variants is provided in the supplemental material.

NCBE Mediates Electroneutral, DIDS-sensitive Na^+-coupled HCO_3^- Transport

Previous reports of NCBE describe the protein as being a Na^+-driven Cl-HCO_3 exchanger. This assignment was based

on the results of two types of functional assays: (*a*) ^{22}Na and ^{36}Cl flux data from oocytes expressing NCBE (20) and (*b*) pH_i measurements on BCECF-loaded mammalian cells that were transfected with NCBE (20, 23). Our results agree with those of others in three major areas as described in the following paragraphs.

NCBE Is a HCO_3^- Transporter—NCBE mediates a pH_i recovery from an acid load only in the presence of HCO_3^- regardless of whether one studies NCBE heterologously expressed in HEK293 cells (20), 3T3 cells (23), or *Xenopus* oocytes (present study, Figs. 3 and Fig. 4).

NCBE Cotransports Na^+ and HCO_3^-—The original report of NCBE demonstrated that oocytes expressing NCBE accumulate ^{22}Na only in the presence of extracellular HCO_3^- (20). The same authors demonstrated that NCBE-expressing HEK293 cells, in the presence of HCO_3^-, are incapable of recovering from an acid load until Na^+ is restored to the bathing medium (20), a result replicated by others in NCBE-expressing 3T3 cells (23) and in the present study in NCBE-expressing oocytes (Fig. 5).

DIDS Blocks NCBE—Others found that NCBE expressed in oocytes mediates a ^{22}Na influx that is blocked by 300 μM DIDS (20). Others also found that, whether expressed in HEK293 cells or 3T3 cells, NCBE mediates a pH_i recovery that is prevented by the addition of 300 μM DIDS to the bathing medium (20, 23). In the present study we demonstrated that 200 μM DIDS is sufficient to block the pH_i recovery mediated by NCBE in oocytes (Fig. 8). The lysine-containing motif "EKLFE," located at the extracellular end of the fifth transmembrane span of human, mouse, and rat NCBE, is predicted to play an important role in this DIDS blockade as has been demonstrated for lysine residues at this position in AE1 (37) and NBCe1 (38).

Another important aspect of NCBE molecular physiology, although never disputed, has actually never been demonstrated, namely that NCBE is an electroneutral transporter. The present study is the first and only to provide direct evidence that HCO_3^- transport mediated by NCBE is electroneutral. If NCBE was electrogenic and working with a 2:1 HCO_3^-:Na^+ stoichiometry, for an oocyte with a membrane resistance of 0.25 megaohm we calculated that NCBE should elicit a hyperpolarization of −26 mV.[9] However, the switch from a CO_2/HCO_3^--free to a CO_2/HCO_3^--containing solution (Fig. 3*A*) did not elicit any rapid changes in the V_m of oocytes expressing NCBE.

NCBE Normally Does Not Couple Net Cl^- Efflux to Net HCO_3^- Influx

As it is not practical to deplete oocytes of intracellular Cl^-, our laboratory has previously assayed the presence *versus* the absence of Na^+-driven Cl-HCO_3 exchange activity by reversing the direction of Na^+-driven Cl-HCO_3 exchange (by removing extracellular Na^+) and then asking whether the subsequent removal of bath Cl^- blocks the Na^+-dependent export of HCO_3^- from the cell (13, 26, 28, 39). In other words, does net HCO_3^- efflux require extracellular Cl^-? However, because we were unable to substantially reverse the direction of NCBE transport by removing bath Na^+ (Fig. 6), this approach is impossible for NCBE-expressing oocytes.

In the present study, we used a blunt tipped Cl^--selective electrode at the oocyte surface to monitor changes in $[Cl^-]_S$, produced by changes in net Cl^- efflux, as we exposed the cell to a CO_2/HCO_3^--containing solution. We validated our experimental approach in four ways.

1) We demonstrated that the exposure to CO_2/HCO_3^- produces a transient increase in $[Cl^-]_S$ for oocytes expressing three known Cl^--coupled HCO_3^- transporters: human AE1, human NDCBE-EGFP, and squid NDCBE (Figs. 9 and 10). Our positive control studies provide the first demonstration that both human and squid NDCBE couple net HCO_3^- influx to a net Cl^- efflux (Figs. 9 and 10), that is, in the physiological direction of transport. The previous work showed that human NDCBE, when operating in the forward direction, mediates a CO_2/HCO_3^--stimulated ^{36}Cl efflux (26), and human and squid NDCBE, when operating in reverse, require extracellular Cl^- (26, 28). 2) We demonstrated the lack of a transient $[Cl^-]_S$ increase for oocytes expressing rat NBCn1-EGFP or oocytes that had been injected with H_2O (Figs. 9 and 10). 3) We prevented the increase in $[Cl^-]_S$ for oocytes expressing AE1 by preincubation with DIDS (Fig. 10). 4) We prevented the transient increase of $[Cl^-]_S$ in oocytes expressing human NDCBE-EGFP by switching the cell to CO_2/HCO_3^- in the absence of bath Na^+ (Fig. 10). Our central observation was that exposure to CO_2/HCO_3^- does not produce a transient increase in $[Cl^-]_S$ for oocytes expressing NCBE-EGFP (Figs. 9 and 10), thereby providing the first demonstration that NCBE does not couple net HCO_3^- influx to a net Cl^- efflux.

NCBE-mediated Net HCO_3^- Influx Does Not Require Extracellular Cl^-

The only area in which our conclusions conflict with those of others concerns whether NCBE, like NDCBE, couples a net efflux of Cl^- to the net influx of HCO_3^-. Others have presented two major arguments in support of the hypothesis that NCBE is a Na^+-driven Cl-HCO_3 exchanger: 1) NCBE transport is Cl^--dependent and 2) NCBE transports ^{36}Cl. We will address the first argument in this section and the second in the following section.

The first argument in support of the hypothesis that NCBE is a Na^+-driven Cl-HCO_3 exchanger is that NCBE transport is Cl^--dependent. In their original report, Wang *et al.* (20) found that removing extracellular Cl^- reduces the NCBE-dependent $^{22}Na^+$ influx into oocytes, during a 15-min incubation period, by ~50% (their Fig. 2a, bar "C" *versus* bar "A"). In their supplemental data they further report that the ^{22}Na influx, during a 35-min incubation period, falls by ~80% in a Cl^--free solution. This result cannot be explained in terms of direct effect (*i.e.* lowering $[Cl^-]_o$ *per se*) on Na^+-driven Cl-HCO_3 exchange activity, which, if anything, should have been stimulated by Cl^- removal. Neither could the inhibition have been the indirect consequence of a substantial depletion of intracellular Cl^- inasmuch as our data show $[Cl^-]_i$ to be stable for at least 15 min

[9] Membrane resistance was determined from voltage clamp experiments on H_2O-injected oocytes such as those in Ref. 27. We assumed an oocyte H_2O content of 0.5 μl (40% of total volume) and calculated an NCBE-mediated J_{HCO_3} of 4.62 μM/s as detailed later under "Discussion."

under comparable conditions (not shown; $\Delta[Cl^-]_i = -1 \pm 1$ mM, $n = 4$). Thus, the aforementioned ^{22}Na data do not prove that NCBE engages in physiological Na^+-driven Cl-HCO_3 exchange activity.

In further studies, Wang *et al.* (20) heterologously expressed NCBE in HEK293 cells and demonstrated that removing bath Cl^- reduces the NCBE-mediated pH_i recovery from an intracellular acid load by ~70%. Again these results are inconsistent with a direct effect (*i.e.* lowering $[Cl^-]_o$ *per se*) on Na^+-driven Cl-HCO_3 exchange activity. Wang *et al.* (20) suggest that the extracellular Cl^- removal led to Cl^- depletion of the cells. However, we note that Cl^- is very difficult to wash out of glomerular mesangial cells (40) and neurons (3). Moreover Cl^- reloads into neurons with great rapidity (3). Although Wang *et al.* (20) preincubated their cells for 1 h in a Cl^--free medium, they did not verify that $[Cl^-]_i$ actually fell. Moreover when they prepulsed their cells with NH_3/NH_4^+ to impose the acid load (41), they reintroduced 40 mM Cl^- (as NH_4Cl) and thereby probably reloaded their cells with Cl^- just before monitoring the pH_i recovery mediated by NCBE. Thus, the aforementioned pH_i recovery data do not prove that NCBE engages in physiological Na^+-driven Cl-HCO_3 exchange activity.

Others, working with 3T3 cells, also report that external Cl^- removal reduces the NCBE-mediated pH_i recovery from an acid load (23). They suggested that Cl^- either directly or indirectly stimulates NCBE. In the present study, albeit in oocytes, we found that removing bath Cl^- does not significantly affect the net HCO_3^- influx (all of which is Na^+-dependent) mediated by NCBE (Fig. 7).

NCBE Mediates DIDS-sensitive Cl^- Self-exchange

The second argument in support of the hypothesis that NCBE is a Na^+-driven Cl-HCO_3 exchanger is that NCBE transports ^{36}Cl. In their original report, Wang *et al.* (20) demonstrate that, in NCBE-expressing oocytes preloaded with ^{36}Cl, the isotope exits most rapidly in the simultaneous presence of extracellular Cl^-, Na^+, and HCO_3^- (their Fig. 2c, bar "A"). Applying DIDS (their Fig. 2c, bar "A + DIDS") or removing bath Na^+ (their bar "B") each inhibits ^{36}Cl efflux by ~45% (they performed no ^{36}Cl efflux experiments on H_2O-injected oocytes). These data would be consistent with Na^+-driven Cl-HCO_3 exchanger activity save for two observations. First, replacing CO_2/HCO_3^- with butyrate (their Fig. 2c, bar "E") reduces ^{36}Cl efflux by ~80% (*versus* only ~45% for either DIDS addition or Na^+ removal). Second, removing bath Cl^- inhibits ^{36}Cl efflux by ~45% (their Fig. 2c, bar "C").

Wang *et al.* (20) interpret the last observation as follows. As discussed above, their supplemental data show that reducing $[Cl^-]_o$ inhibits the ^{22}Na influx mediated by NCBE. Thus, they suggest that the external Cl^- dependence of ^{36}Cl efflux (their Fig. 2c, bar "C") reflects the dependence of net transport by NCBE on external Cl^-. However, we found that reducing $[Cl^-]_o$ to 0 mM (see previous section and Fig. 7) has no discernable effect on net HCO_3^- transport, ruling out a significant modulatory role for external Cl^-. Therefore, we suggest that the trans-side Cl^- dependence of ^{36}Cl efflux in the experiments of Wang *et al.* (20) indicates that about half of the total ^{36}Cl efflux represents a Cl-Cl exchange. In light of our further observation that NCBE does not couple net HCO_3^- influx to net Cl^- efflux (Figs. 9 and 10), the most straightforward explanation for the ^{36}Cl efflux data of Wang *et al.* (20) is that although NCBE does not mediate net Cl^- transport, it mediates a DIDS-sensitive Cl-Cl exchange. Indeed Wang *et al.* (20) note that ^{36}Cl movement is bidirectional inasmuch as NCBE-expressing oocytes also mediate Cl^- influx when bathed in a Na^+- and HCO_3^--containing solution (their Fig. 2b, bar "A").

Using a similar ^{36}Cl efflux assay, which we validated using oocytes expressing NDCBE as a positive control and H_2O-injected oocytes as a negative control, we demonstrated that enhanced ^{36}Cl efflux from NCBE-expressing oocytes occurs in both our Na^+-containing (Fig. 11*B*, *bar F*) and our Na^+-free (Fig. 11*B*, *bar G*) CO_2/HCO_3^- solutions. Note that the Na^+-free condition is one under which NCBE is inactive with regard to net HCO_3^- transport (Figs. 5 and 6). Moreover enhanced ^{36}Cl efflux from NCBE-expressing oocytes was negated in our Na^+- and Cl^--free solution (Fig. 11*B*, *bar I*). Thus, the trans-side dependence of ^{36}Cl efflux on bath Cl^- allows us to conclude that, in the absence of bath Na^+, all CO_2/HCO_3^--stimulated ^{36}Cl efflux represents Cl-Cl exchange. Furthermore because our $[Cl^-]_S$ data in Figs. 9 and 10 show that NCBE does not mediate net Cl^- efflux in the presence of bath Na^+ and Cl^-, we can conclude that, in the presence of bath Na^+ and Cl^-, all CO_2/HCO_3^--stimulated ^{36}Cl efflux represents Cl-Cl exchange as well.

The surprising observation was that, in the absence of bath Cl^-, bath Na^+ supports a small but significant CO_2/HCO_3^--stimulated ^{36}Cl efflux (Fig. 11*B*, *bar I versus bar H*). Note that this flux, which is consistent with Na^+-driven Cl-HCO_3 exchange activity, occurs only under highly nonphysiological conditions: the complete absence of extracellular Cl^-.

From the CO_2-induced pH_i decreases in the present study, we computed a mean intrinsic intracellular buffering power (42) of 18 ± 2 mM/pH unit ($n = 7$ NCBE-expressing oocytes). Given a mean pH_i of 6.8 during a pH_i recovery, the computed open system CO_2/HCO_3^- buffering power (42) is ~15 mM/pH unit for a total intracellular buffering power of ~33 mM/pH unit. Because the average pH_i recovery rate for NCBE-expressing oocytes in CO_2/HCO_3^- was 14×10^{-5} pH units/s, we estimated that the rate of net HCO_3^- influx into an NCBE-expressing oocyte is 4.62 μM/s. Given that the $[Cl]_i$ of NCBE-expressing oocytes is 40 mM and that 21% of oocyte Cl^- exits during a 30-min incubation in Cl^--free CO_2/HCO_3^- solution *versus* 10% during a 30-min incubation in Cl^--free ND96, we estimated that the Cl^- efflux is 2.44 μM/s. The ratio of the HCO_3^- entry to Cl^- exit is ~1.9 *versus* the predicted 2.0 for Na^+-driven Cl-HCO_3 exchange. Thus, under the highly nonphysiological conditions in which Cl^- is absent from the bath, we can account for all of the Cl^- efflux by Na^+-driven Cl-HCO_3 exchange.

Thus, our data indicate the following. 1) For $[Cl^-]_o \geq 10$ mM, and thus under physiological conditions, NCBE engages parallel Cl-Cl exchange plus electroneutral Na/HCO_3 cotransport but no Na^+-driven Cl-HCO_3 exchange activity. 2) For $[Cl^-]_o = 0$, NCBE can now enter a nonphysiological mode in which it mediates Na^+-driven Cl-HCO_3 exchange possibly with parallel electroneutral Na/HCO_3 cotransport.

How do we interpret *bar F versus bar H* in Fig. 11*B*? Under the conditions of *bar F* ($[Cl^-]_o$ = 101 mM) all of the CO_2/HCO_3^--stimulated ^{36}Cl efflux is Cl-Cl exchange. Under the conditions of *bar H* ($[Cl^-]_o$ = 0), all the Cl-Cl exchange halts and is replaced by a smaller degree of Na^+-driven Cl-HCO_3 exchange. We emphasize that removing bath Cl^- (*i.e.* the transition from the condition of *bar F* to *bar H* in Fig. 11*B*) does not reduce net HCO_3^- uptake (Fig. 7).

Regarding NDCBE, in their 2001 study, Grichtchenko *et al.* (26) concluded that more than 80% of the ^{36}Cl efflux mediated by NDCBE represents Cl-Cl exchange. Compared with the oocytes and/or conditions used in that previous study, we found that the present HCO_3^- efflux is greater, whereas the present ^{36}Cl flux is lesser so that the present computed HCO_3^-:Cl^- flux ratio is almost exactly the 2:1 predicted for Na^+-driven Cl-HCO_3 exchange. In other words, for the oocytes and/or conditions in the present study, we can account for all of the ^{36}Cl efflux of NDCBE by Na^+-driven Cl-HCO_3 exchange under physiological conditions (*i.e.* Fig. 11*A*, *bar F*). Our surface $[Cl^-]$ data showed that with bath $[Cl^-]$ as low as 10 mM NDCBE still mediates a net Cl^- efflux (Figs. 9 and 10). However, our ^{36}Cl data showed that the complete removal of bath Cl^- reduces the ^{36}Cl efflux to background levels (Fig. 11*A*, *bar H versus bar F*). The most straightforward explanations for this observation are that 1) Na^+-driven Cl-HCO_3 exchange by NDCBE requires that Cl^- bind to an extracellular Cl^- modifier site (43) or 2) removal of bath Cl^- causes NDCBE to shift from Na^+-driven Cl-HCO_3 exchange to electroneutral Na/HCO_3 cotransport.

It is interesting to note that the γ-aminobutyric acid transporter GAT-1, like NCBE, engages in futile Cl-Cl exchange. In the absence of Cl^-, GAT-1 cotransports 2 Na^+/1 γ-aminobutyric acid, but in the presence of Cl^-, the transporter imports 1 Na^+/1 Cl^-/1 γ-aminobutyric acid in exchange for 1 Cl^- (44). The involvement of Cl^- in the transport cycle increases the affinity of GAT-1 for Na^+ (44). It is possible that extracellular Cl^- also raises the affinity of NCBE for one of its substrates (*i.e.* Na^+ or HCO_3^-). However, we note that removing bath Cl^- did not reduce net HCO_3^- uptake by NCBE (Fig. 7) under the conditions of our assay with the transporter, without its natural posttranslational modifications or binding partners, heterologously expressed in *Xenopus* oocytes.

Conclusion

We conclude that NCBE, unlike NDCBE, does not under physiological conditions perform the Na^+-driven Cl-HCO_3 exchange activity for which it was named. Instead NCBE, like NBCn1, mediates an electroneutral Na/HCO_3 cotransport activity with an associated function. In the case of NBCn1, this associated function is a Na^+ conductance (13); in the case of NCBE, this associated function is likely a futile Cl-Cl exchange. We therefore propose that NCBE be renamed NBCn2.

Implications

If our results in oocytes translate to mammalian cells, the reassignment of the ionic mechanism of SLC4A10 may have important implications for cells expressing the transporter. First, by not engaging in net Cl^- transport, NBCn2 could operate without altering the equilibrium potential for Cl^-, which could be important for stabilizing inhibitory postsynaptic currents. Second, by transporting only one HCO_3^- for each Na^+, NBCn2 would be less energy-efficient than NDCBE, the price paid for 1) not altering $[Cl^-]_i$ and yet remaining electroneutral and 2) being theoretically capable of taking up HCO_3^- against a relatively steep gradient.

Acknowledgments—At Yale University, we thank Bruce Davis, Chiyoko Kobayashi, and Andrew Dai for technical assistance. We thank Duncan Wong for computer support, Liming Chen for providing cRNA, and Cecilia Canessa and co-workers for providing Xenopus oocytes. At Case Western Reserve University, we thank Andrea Romani for providing ^{36}Cl.

REFERENCES

1. Romero, M. F., Fulton, C. M., and Boron, W. F. (2004) *Pfluegers Arch. Eur. J. Physiol.* **447,** 495–509
2. Parker, M. D., and Boron, W. F. (2007) in *Seldin and Giebisch's The Kidney: Physiology and Pathophysiology* (Hebert, S. C., and Alpern, R. J., eds) pp. 1481–1497, Academic Press, Burlington, MA
3. Schwiening, C. J., and Boron, W. F. (1994) *J. Physiol.* (*Lond.*) **475,** 59–67
4. Praetorius, J., Nejsum, L. N., and Nielsen, S. (2004) *Am. J. Physiol.* **286,** C601–C610
5. Praetorius, J., and Nielsen, S. (2006) *Am. J. Physiol.* **291,** C59–C67
6. Waldmann, R., Champigny, G., Bassilana, F., Heurteaux, C., and Lazdunski, M. (1997) *Nature* **386,** 173–177
7. Pasternack, M., Smirnov, S., and Kaila, K. (1996) *Neuropharmacology* **35,** 1279–1288
8. Eiden, L. E., Schafer, M. K., Weihe, E., and Schutz, B. (2004) *Pfluegers Arch. Eur. J. Physiol.* **447,** 636–640
9. Jarolimek, W., Misgeld, U., and Lux, H. D. (1990) *Pfluegers Arch. Eur. J. Physiol.* **416,** 247–253
10. Ransom, B. R. (1992) *Prog. Brain Res.* **94,** 37–46
11. Spray, D. C., Harris, A. L., and Bennett, M. V. L. (1981) *Science* **211,** 712–715
12. Pushkin, A., Abuladze, N., Lee, I., Newman, D., Hwang, J., and Kurtz, I. (1999) *J. Biol. Chem.* **274,** 16569–16575
13. Choi, I., Aalkjær, C., Boulpaep, E. L., and Boron, W. F. (2000) *Nature* **405,** 571–575
14. Bourgeois, S., Masse, S., Paillard, M., and Houillier, P. (2002) *Am. J. Physiol.* **282,** F655–F668
15. Odgaard, E., Jakobsen, J. K., Frische, S., Praetorius, J., Nielsen, S., Aalkjær, C., and Leipziger, J. (2004) *J. Physiol.* (*Lond.*) **555,** 205–218
16. Boron, W. F., and Russell, J. M. (1983) *J. Gen. Physiol.* **81,** 373–399
17. Russell, J. M., and Boron, W. F. (1976) *Nature* **264,** 73–74
18. Thomas, R. C. (1977) *J. Physiol.* (*Lond.*) **273,** 317–338
19. Boron, W. F. (1977) *Am. J. Physiol.* **233,** C61–C73
20. Wang, C. Z., Yano, H., Nagashima, K., and Seino, S. (2000) *J. Biol. Chem.* **275,** 35486–35490
21. Sebat, J., Lakshmi, B., Malhotra, D., Troge, J., Lese-Martin, C., Walsh, T., Yamrom, B., Yoon, S., Krasnitz, A., Kendall, J., Leotta, A., Pai, D., Zhang, R., Lee, Y. H., Hicks, J., Spence, S. J., Lee, A. T., Puura, K., Lehtimaki, T., Ledbetter, D., Gregersen, P. K., Bregman, J., Sutcliffe, J. S., Jobanputra, V., Chung, W., Warburton, D., King, M. C., Skuse, D., Geschwind, D. H., Gilliam, T. C., Ye, K., and Wigler, M. (2007) *Science* **316,** 445–449
22. Jacobs, S., Ruusuvuori, E., Sipila, S. T., Haapanen, A., Damkier, H. H., Kurth, I., Hentschke, M., Schweizer, M., Rudhard, Y., Laatikainen, L. M., Tyynela, J., Praetorius, J., Voipio, J., and Hubner, C. A. (2008) *Proc. Natl. Acad. Sci. U. S. A.* **105,** 311–316
23. Giffard, R. G., Lee, Y. S., Ouyang, Y. B., Murphy, S. L., and Monyer, H. (2003) *Eur. J. Neurosci.* **18,** 2935–2945
24. Choi, I., Rojas, J. D., Kobayashi, C., and Boron, W. F. (2002) *FASEB J.* **16,** A796
25. Groves, J. D., and Tanner, M. J. (1992) *J. Biol. Chem.* **267,** 22163–22170
26. Grichtchenko, I. I., Choi, I., Zhong, X., Bray-Ward, P., Russell, J. M., and Boron, W. F. (2001) *J. Biol. Chem.* **276,** 8358–8363

27. Toye, A. M., Parker, M. D., Daly, C. M., Lu, J., Virkki, L. V., Pelletier, M. F., and Boron, W. F. (2006) *Am. J. Physiol.* **291,** C788–C801
28. Virkki, L. V., Choi, I., Davis, B. A., and Boron, W. F. (2003) *Am. J. Physiol.* **285,** C771–C780
29. Chen, L. M., Kelly, M. L., Rojas, J., Parker, M. D., Gill, H. S., Davis, B. A., and Boron, W. F. (2008) *Neuroscience* **151,** 374–385
30. Romero, M. F., Fong, P., Berger, U. V., Hediger, M. A., and Boron, W. F. (1998) *Am. J. Physiol.* **274,** F425–F432
31. Virkki, L. V., Wilson, D. A., Vaughan-Jones, R. D., and Boron, W. F. (2002) *Am. J. Physiol.* **282,** C1278–C1289
32. Barish, M. E. (1983) *J. Physiol.* (*Lond.*) **342,** 309–325
33. Humphreys, B. D., Jiang, L., Chernova, M. N., and Alper, S. L. (1994) *Am. J. Physiol.* **267,** C1295–C1307
34. Doughty, J. M., and Langton, P. D. (2001) *J. Physiol.* (*Lond.*) **534,** 753–761
35. Kietz, D., Bartel, D., Lepke, S., and Passow, H. (1991) *Biochim. Biophys. Acta* **1064,** 81–88
36. Hubner, C. A., Hentschke, M., Jacobs, S., and Hermans-Borgmeyer, I. (2004) *Gene Expr. Patterns* **5,** 219–223
37. Okubo, K., Kang, D., Hamasaki, N., and Jennings, M. L. (1994) *J. Biol. Chem.* **269,** 1918–1926
38. Lu, J., and Boron, W. F. (2007) *Am. J. Physiol.* **292,** C1787–C1798
39. Piermarini, P. M., Choi, I., and Boron, W. F. (2007) *Am. J. Physiol.* **292,** C2032–C2045
40. Boyarsky, G., Ganz, M. B., Sterzel, B., and Boron, W. F. (1988) *Am. J. Physiol.* **255,** C857–C869
41. Boron, W. F., and De Weer, P. (1976) *J. Gen. Physiol.* **67,** 91–112
42. Roos, A., and Boron, W. F. (1981) *Physiol. Rev.* **61,** 296–434
43. Dalmark, M. (1976) *J. Gen. Physiol.* **67,** 223–234
44. Loo, D. D., Eskandari, S., Boorer, K. J., Sarkar, H. K., and Wright, E. M. (2000) *J. Biol. Chem.* **275,** 37414–37422